

Ground-state bands and excitation modes in  $^{183}\text{Hg}$ 

D. T. Shi,<sup>1</sup> W. C. Ma,<sup>2,1,\*</sup> A. V. Ramayya,<sup>1</sup> J. H. Hamilton,<sup>1</sup> B. R. S. Babu,<sup>1</sup>  
 J. Kormicki,<sup>1,†,‡</sup> L. Chaturvedi,<sup>1,§</sup> Q. H. Lu,<sup>1</sup> L. T. Brown,<sup>1</sup>  
 S. L. Tabor,<sup>3</sup> M. A. Riley,<sup>3</sup> J. Döring,<sup>3</sup> D. E. Archer,<sup>3</sup> T. Brown,<sup>3</sup>  
 S. K. Jewell,<sup>3</sup> R. A. Kaye,<sup>3</sup> O. J. Tekyi-Mensah,<sup>3</sup> and P. B. Semmes<sup>4</sup>

<sup>1</sup>Department of Physics, Vanderbilt University, Nashville, Tennessee 37235

<sup>2</sup>Department of Physics, Mississippi State University, Mississippi State, Mississippi 39762

<sup>3</sup>Department of Physics, Florida State University, Tallahassee, Florida 32306

<sup>4</sup>Department of Physics, Tennessee Technological University, Cookeville, Tennessee 38505

(Received 16 November 1994)

A new in-beam study of  $^{183}\text{Hg}$  levels has been carried out by using the  $^{155}\text{Gd}(^{32}\text{S}, 4n)$  reaction at a beam energy of 160 MeV. A new pair of signature-partner bands, with large signature splitting, has been established in  $^{183}\text{Hg}$ . The bandhead of these signature-partner bands is assigned to be the ground state of  $^{183}\text{Hg}$  with a configuration of  $1/2^- [521]$ . The measured ratios of directional correlations (DCO ratios) revealed decay patterns for the proposed  $9/2^+ [624]$  bands in  $^{183}\text{Hg}$  different from those of  $^{185}\text{Hg}$ .

PACS number(s): 27.70.+q, 21.10.Hw, 23.20.-g

The ground states of the light even-even mercury nuclei ( $A \leq 188$ ) [1] exhibit slight oblate deformation ( $\beta \approx -0.15$ ), but low-lying excited bands associated with prolate deformation of  $\beta \approx 0.25$  quickly become yrast. On the other hand, isotope shift experiments indicate that the nuclear charge radii of the ground state of odd- $A$   $^{181-185}\text{Hg}$  are as large as that of  $^{196}\text{Hg}$  [2]. Such a drastic effect implies a very strong driving force of the odd particle toward a well-deformed shape as  $A$  decreases below 187. The investigations of these odd- $A$  nuclei can provide important information on the one-quasiparticle excitations to serve as a basis for constructing the multiquasiparticle states which are responsible for the excitations in the neighboring even-even nuclei.

Rotational bands built on both oblate and prolate structures have been established for  $^{185}\text{Hg}$  [3]. Recently two pairs of rotational bands were identified for the first time in  $^{183}\text{Hg}$  by using the fragment mass analyzer (FMA) and a ten Compton-suppressed Ge detector array at the target position at Argonne National Laboratory (ANL) [4]. Both mass- $\gamma$  and  $\gamma$ - $\gamma$  coincidence events were collected. However, only  $12 \times 10^6$   $\gamma$ - $\gamma$  coincidence events were obtained. Some weak transitions could not be placed in the level scheme even though they were associated with mass 183 from the mass-gated  $\gamma$ -ray spectrum. No angular distribution or correlation information was obtained for spin and parity assignments. Furthermore, the  $1/2^- [521]$  ground-state band seen in  $^{185}\text{Hg}$  was not observed in  $^{183}\text{Hg}$ .

Therefore, we carried out a  $\gamma$ - $\gamma$ ,  $\gamma$ - $X$  coincidence experiment at the Florida State University (FSU) tandem-linac facility. The  $^{183}\text{Hg}$  nuclei were populated by bombarding a self-supporting  $^{155}\text{Gd}$  enriched target (2 mg/cm<sup>2</sup> thick) with 160 MeV  $^{32}\text{S}$  beam. The coincident  $\gamma$  rays were measured with ten Compton-suppressed Ge detectors in the Pittsburgh-FSU array and a low energy photon spectrometer (LEPS). The Ge detectors were located at three different angles ( $35^\circ$ ,  $90^\circ$ , and  $145^\circ$ ) with respect to the beam direction. In addition, a group of 28 BGO detectors served as a multiplicity filter. A total of  $80 \times 10^6$  coincidence events were collected and sorted into a matrix, which was added together with the  $\gamma$ - $\gamma$  coincidence matrix obtained from the experiment at ANL. With the requirement of multiplicity  $\geq 2$  in the BGO multiplicity filter to suppress the low multiplicity events, a second coincidence matrix (with  $40 \times 10^6$  coincidence events) also was built. This matrix was used primarily in the later analysis to build the new level scheme as the spectra from this matrix have better peak-to-background ratios than those from the matrix without a multiplicity requirement. A third coincidence matrix also was built between the x rays collected with the LEPS and the  $\gamma$  rays collected with the Ge detectors. In addition another coincidence matrix was built to analyze the directional correlation information (DCO ratio) for spin and parity assignments. In this matrix the  $\gamma$  rays collected by the  $90^\circ$  detectors were sorted onto one axis and those collected by other detectors (located at  $35^\circ$  and  $145^\circ$ ) onto another axis. The extracted DCO ratios of one group of  $\gamma$  rays in  $^{183}\text{Hg}$  were centered at 1.0 and that of another group at 0.6. They were assumed to correspond to stretched  $E2$  and  $M1$  transitions, respectively. The measured  $\gamma$ -ray intensities and DCO ratios are listed in Table I.

Based on  $\gamma$ -ray coincidence relationships, DCO ratios, and  $\gamma$ -ray intensities, a new level scheme has been estab-

\*Present address: Mississippi State University, Mississippi State, MS 39762.

†Also at UNISOR, ORISE, Oak Ridge, TN 37831.

‡On leave from Institute of Nuclear Physics, Cracow, Poland.

§On leave from Banares Hindu University, Banares, India.

TABLE I.  $^{183}\text{Hg}$   $\gamma$ -ray energies, relative intensities (in percentage), DCO ratios, adopted multipolarities, spin assignments, and band labels.

$E_\gamma$ (keV) <sup>a</sup>	Rel. Int. <sup>b</sup>	DCO Ratio	Multip.	Assignment	Band
86.5	1.3(0.2)		(M1)	$3/2 \rightarrow 1/2$	2
88.9	3.8(0.6)	1.1(0.3)	E2	$5/2 \rightarrow 1/2$	1
104.9	29(3)	0.8(0.3)	M1	$(9/2) \rightarrow (7/2)$	4 $\rightarrow$ 3
146.4	5(1)	0.8(0.4)	M1	$(11/2) \rightarrow (9/2)$	3 $\rightarrow$ 4
155.1	1.5(0.2)	0.7(0.2)	M1	$(13/2) \rightarrow (11/2)$	4 $\rightarrow$ 3
178.7	1.0(0.1)	0.7(0.3)	M1	$(15/2) \rightarrow (13/2)$	3 $\rightarrow$ 4
191.4	4(2)	0.8(0.3) <sup>c</sup>	M1	$7/2 \rightarrow 5/2$	2 $\rightarrow$ 1
193.3	1.2(0.2)	0.7(0.3)	M1	$(17/2) \rightarrow (15/2)$	4 $\rightarrow$ 3
194.1	10(2)	0.8(0.2) <sup>c</sup>	E2	$7/2 \rightarrow 3/2$	2
198.9	13(2)	1.0(0.1)	E2	$9/2 \rightarrow 5/2$	1
251.3	20(2)	0.9(0.3)	E2	$(11/2) \rightarrow (7/2)$	3
271.0	13(1)	0.4(0.1)	M1	$(19/2) \rightarrow (17/2)$	5 $\rightarrow$ 6
273.2	Weak		(M1)	$11/2 \rightarrow 9/2$	2 $\rightarrow$ 1
280.4	6.9(0.4)	1.0(0.2)	E2	$11/2 \rightarrow 7/2$	2
290.8	11.4(0.5)	0.8(0.2)	E2	$13/2 \rightarrow 9/2$	1
301.5	19(3)	0.9(0.1)	E2	$(13/2) \rightarrow (9/2)$	4
303.0	7.8(0.8)	0.6(0.2)	M1	$(23/2) \rightarrow (21/2)$	5 $\rightarrow$ 6
333.8	17(1)	1.0(0.2)	E2	$(15/2) \rightarrow (11/2)$	3
346.1	Weak		(M1)	$15/2 \rightarrow 13/2$	2 $\rightarrow$ 1
346.3	13(1)	1.0(0.3)	E2	$(19/2) \rightarrow (15/2)$	5
353.8	20(2)	0.5(0.2)	M1	$(15/2) \rightarrow (13/2)$	5 $\rightarrow$ 7
361.9	3.6(0.6)	0.4(0.2)	M1	$(27/2) \rightarrow (25/2)$	5 $\rightarrow$ 6
363.7	4.5(0.4)	1.1(0.3)	E2	$15/2 \rightarrow 11/2$	2
372.0	13.0(0.5)	0.9(0.2)	E2	$(17/2) \rightarrow (13/2)$	4
375.4	10.8(0.5)	1.1(0.2)	E2	$17/2 \rightarrow 13/2$	1
403.3	66(3)	1.0(0.2)	E2	$(21/2) \rightarrow (17/2)$	6
406.7	10.7(0.7)	0.9(0.2)	E2	$(19/2) \rightarrow (15/2)$	3
422.6	3(2)	0.6(0.2)	M1	$(31/2) \rightarrow (29/2)$	5 $\rightarrow$ 6
429.0	100	1.1(0.2)	E2	$(17/2) \rightarrow (13/2)$	6 $\rightarrow$ 7
435.3	10(3)	1.0(0.4)	E2	$(23/2) \rightarrow (19/2)$	5
438.5	3.9(0.4)	1.1(0.4)	E2	$19/2 \rightarrow 15/2$	2
439.5	9.1(0.5)	0.8(0.2)	E2	$(21/2) \rightarrow (17/2)$	4
450.9	6.7(0.5)	1.0(0.3)	E2	$21/2 \rightarrow 17/2$	1
454.0	47(2)	0.9(0.2)	E2	$(25/2) \rightarrow (21/2)$	6
472.2	8.7(0.7)	1.1(0.4)	E2	$(23/2) \rightarrow (19/2)$	3
500.8	7.0(0.5)	1.1(0.3)	E2	$(25/2) \rightarrow (21/2)$	4
503.4	2.6(0.3)	1.2(0.4)	E2	$23/2 \rightarrow 19/2$	2
512.8	5.5(0.5)	0.8(0.4)	E2	$(27/2) \rightarrow (23/2)$	5
516.3	5.4(0.5)	1.1(0.3)	E2	$25/2 \rightarrow 21/2$	1
521.0	29(2)	1.2(0.3)	E2	$(29/2) \rightarrow (25/2)$	6
531.4	7.8(0.7)	1.0(0.3)	E2	$(27/2) \rightarrow (23/2)$	3
555.3	5.6(0.5)	0.8(0.3)	E2	$(29/2) \rightarrow (25/2)$	4
558.9	2.1(0.3)	1.1(0.5)	E2	$27/2 \rightarrow 23/2$	2
570.2	3.9(0.4)	1.0(0.4)	E2	$29/2 \rightarrow 25/2$	1
581.1	2.8(0.4)	0.9(0.5)	E2	$(31/2) \rightarrow (27/2)$	5
582.7	25(2)	1.0(0.4)	E2	$(33/2) \rightarrow (29/2)$	6
584.6	3.5(0.6)	1.0(0.5)	E2	$(31/2) \rightarrow (27/2)$	3
601.8	1.1(0.2)	1.3(0.9)	E2	$31/2 \rightarrow 27/2$	2
602.2	2.3(0.4)	1.0(0.5)	E2	$(33/2) \rightarrow (29/2)$	4
609.6	2.6(0.4)	0.8(0.4)	E2	$33/2 \rightarrow 29/2$	1
621.9	0.7(0.2)		(E2)	$(35/2) \rightarrow 31/2$	2
626.3	2(1)		(E2)	$(37/2) \rightarrow 33/2$	1
631.5	1.7(0.8)	1.2(0.9)	(E2)	$(35/2) \rightarrow (31/2)$	3
636.6	Weak		(E2)	$(39/2) \rightarrow (35/2)$	2
637.0	13(2)	1.1(0.5)	(E2)	$(37/2) \rightarrow (33/2)$	6
638.0	1.0(0.3)		(E2)	$(37/2) \rightarrow (33/2)$	4
639.9	1(1)		(E2)	$(41/2) \rightarrow (37/2)$	1

TABLE I. (*Continued.*)

$E_\gamma$ (keV) <sup>a</sup>	Rel. Int. <sup>b</sup>	DCO Ratio	Multip.	Assignment	Band
641.3	1.1(0.3)	1.0(0.7)	(E2)	(35/2) → (31/2)	5
668.8	0.3(0.3)		(E2)	(39/2) → (35/2)	3
683.1	8(3)		(E2)	(41/2) → (37/2)	6
692.9	0.6(0.3)		(E2)	(39/2) → (35/2)	5
723.1	4(1)		(E2)	(45/2) → (41/2)	6
729.0	0.6(0.3)		(E2)	(43/2) → (39/2)	5

<sup>a</sup>The errors in the energies of these gamma rays are about 0.2 keV except for weak gamma rays where the errors could be as large as 0.5 keV.

<sup>b</sup>Gamma-ray relative intensities, without internal conversion correction, were extracted from the gamma-gamma coincidence matrix with the requirement of multiplicity  $\geq 2$  in the BGO multiplicity filter, and the mass-183 gated gamma spectra. "Weak" means that the peaks are too weak to obtain accurate fits.

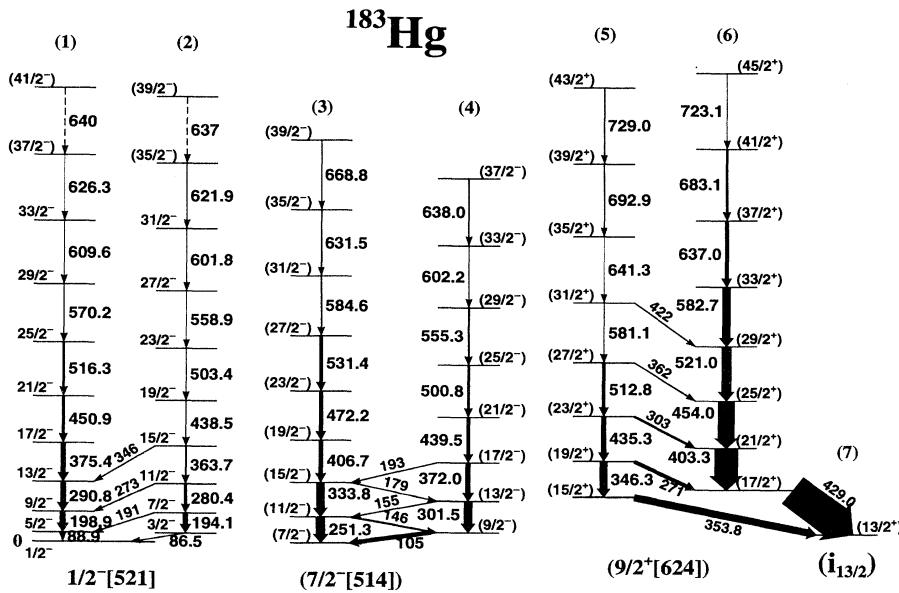
<sup>c</sup>The 191.4-keV and 194.1-keV transitions cannot be well separated.

lished for  $^{183}\text{Hg}$  as shown in Fig. 1. The two pairs of previously known bands (bands 3, 4 and 5, 6) [4] were proposed to be built on the  $7/2^-$  [514] and  $9/2^+$  [624] orbitals based on the systematics of the Nilsson orbitals in this mass region, and by comparison with  $^{185}\text{Hg}$ . One additional high-spin state was observed in bands 3, 5, and 6 in the present investigation. Bands 1 and 2 were unknown before. Each one of them consists of stretched E2 transitions and the two bands are connected by M1 interband transitions. Figure 2 shows the sum-gate spectra of these two bands and their coincidence relationship with mercury K x rays. The stronger transitions (198.9- and 194.1-keV) in these two bands can be seen in the mass-183 gated  $\gamma$ -ray spectrum obtained in the previous experiment. Therefore, these bands are assigned to  $^{183}\text{Hg}$ . The ground-state spin and parity of  $^{183}\text{Hg}$  have been established to be  $1/2^-$  in an optical pumping experiment [5]. The new bands are suggested to be built on the  $1/2^-$  [521] ground-state configuration, the same

assignment, as made for the ground state in  $^{185}\text{Hg}$  [3].

From the optical pumping experiments, the ground states of  $^{181,183,185}\text{Hg}$  have been found to be strongly prolate deformed [2]. The moments of inertia of bands 1 and 2 are consistent with the expected prolate shape. The large signature splitting as shown in Fig. 3, persisting up to the highest spins observed, is also expected for the  $1/2^-$  [521] orbital. These properties and the energies of the  $\gamma$  rays in these two bands fit very well with the systematics of the  $N = 103$  isotones, such as  $^{181}\text{Pt}$  [6] and  $^{179}\text{Os}$  [7]. The angular momentum alignment is very gradual at lower rotational frequencies in these bands, but suddenly increases as the rotational frequency approaches 0.3 MeV (see Fig. 4). In  $^{185}\text{Hg}$  the unfavored signature of this ground-state configuration was not found [3] presumably because of its weak population.

Bands 1 and 2 are observed up to a quite high spin ( $39/2^-$ ) considering that the strongest transitions in these two bands have relative intensities of only about

FIG. 1. The  $^{183}\text{Hg}$  level scheme.

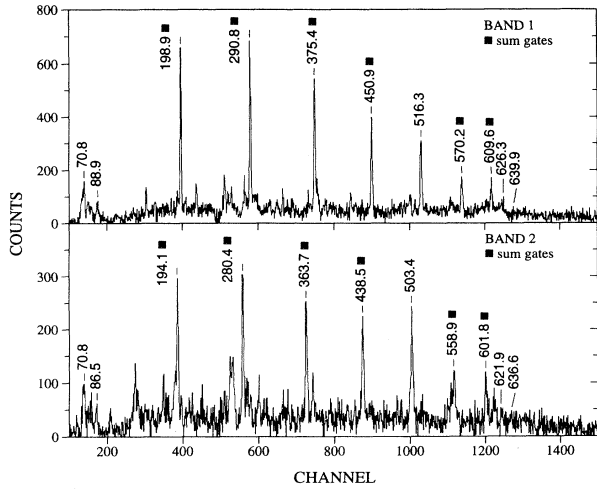


FIG. 2. Sum-gate spectra of bands 1 and 2. The gates with energies marked by squares were used in the sum. All energies are in keV.

10% of the 429-keV transition, the strongest one in the level scheme. The intensity of the 251.3-keV  $\gamma$  ray, the strongest transition in bands 3 and 4, is  $\sim 20\%$ . At higher spins,  $\gamma$ -ray intensities drop abruptly in all bands observed. Thus the previously known bands could be extended to only one higher spin state. This is related to the strong competition from fission at higher excitation energy in the very neutron deficient  $^{183}\text{Hg}$ .

The spins and parities of the other band heads (bands 3–6) cannot be determined experimentally as the transitions linking those levels to the ground state are not observed. Even though the in-band and interband transitions in these bands have DCO ratios consistent with

stretched  $E2$  and  $M1$  transitions, respectively, we have to put the spin and parity assignments for all levels in these bands in parentheses.

The weakly oblate deformed  $i_{13/2}^+$  isomeric state and rotational band built on it were observed in several heavier Hg isotopes including  $^{185}\text{Hg}$ . The  $9/2^+[624]$  prolate structure also decays to this isomeric state. Such an oblate isomeric state should exist in  $^{183}\text{Hg}$  but has not been found experimentally. Bindra *et al.* [4] suggested the 354-keV transition in  $^{183}\text{Hg}$  as the only observed band member built on the  $i_{13/2}^+$  state. However, our new DCO ratio data indicate that the 353.8-keV transition is an  $M1$  transition instead of an  $E2$ , and the 346.3-keV transition is  $E2$  rather than  $M1$  as assumed previously [4]. Therefore, the 346.3-keV transition is a band member in band 5, and the 353.8 keV is an interband transition between band 5 and the isomeric state rather than a band member of the suggested oblate configuration built on the isomeric state. The lowest transition associated with band 6 has an energy of 429 keV, and the one just above it has a smaller energy, 403 keV, while the other transitions at higher spins follow a pattern of energies of a rotational band. This indicates that the 429-keV transition is not a member of band 6, but is a transition to the oblate  $i_{13/2}$  isomeric state.

The bands assigned  $9/2^+[624]$  configuration in  $^{185}\text{Hg}$  and the  $N = 103$  isotone  $^{181}\text{Pt}$  have the largest population intensities. Likewise bands 5 and 6 are populated with the largest intensities. Large signature splitting is observed for these two bands as can be seen from Fig. 3. This is not expected for high- $K$  bands in a symmetrically deformed potential. A possible explanation for the strong signature splitting may come from the hexadecapole deformation or asymmetric deformation ( $\gamma$  degree of freedom). An alternative explanation may be the mixing of the wave function of the  $9/2^+[624]$  with the oblate structure of the same  $\nu i_{13/2}$  subshell. The prolate-oblate shape coexistence is observed in nearby even and odd- $A$  Hg isotopes. Our new findings from DCO ratio measurements do not alter our previous interpretations of the configurations of bands 5, 6, and 7. However, they do indicate a difference in the decay patterns of the proposed  $9/2^+[624]$  configuration in  $^{183}\text{Hg}$  from that in  $^{185}\text{Hg}$ . The  $(15/2^+)$  level of band 5 in  $^{183}\text{Hg}$  decays to the  $(13/2^+)$  isomeric state, while in  $^{185}\text{Hg}$  this band continues its decay sequence down to the lowest level of this configuration, the  $9/2^+$  bandhead, thus indicating less interaction with the oblate structure. If an oblate structure above the  $(13/2^+)$  isomeric state exists in  $^{183}\text{Hg}$ , it must be more weakly populated than in  $^{185}\text{Hg}$ .

Bands 3 and 4 were proposed to be the  $7/2^- [514]$  configuration [4], based primarily on the almost identical transition energies between these bands and the  $7/2^- [514]$  bands in  $^{185}\text{Hg}$  [3]. The  $B(M1; I \rightarrow I - 1)/B(E2; I \rightarrow I - 2)$  ratios have been derived for bands 3 and 4 from the experimental  $\gamma$ -ray intensities under the assumption that the  $I \rightarrow I - 1$  transitions are pure  $M1$  transitions (and therefore these values are upper limits). The resulting experimental values vary from 0.18 to 0.09  $\mu_N^2/e^2b^2$  and are shown in Fig. 5. Also shown are simple estimates obtained from the strong

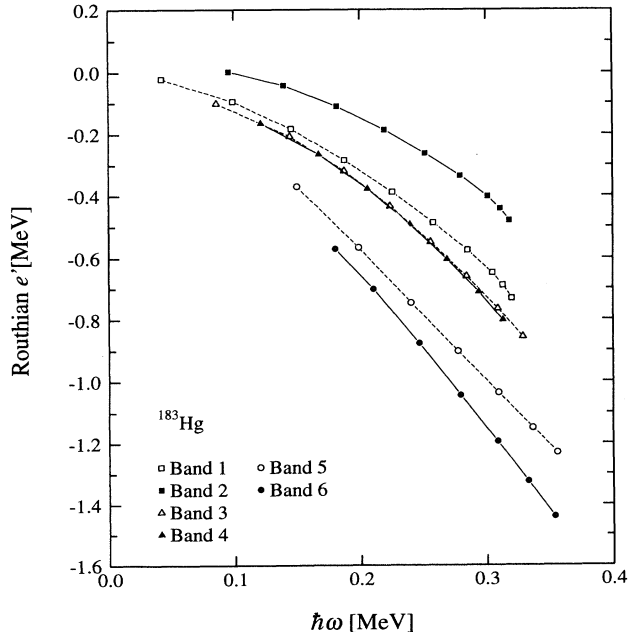


FIG. 3. Experimental Routhians of bands in  $^{183}\text{Hg}$ .

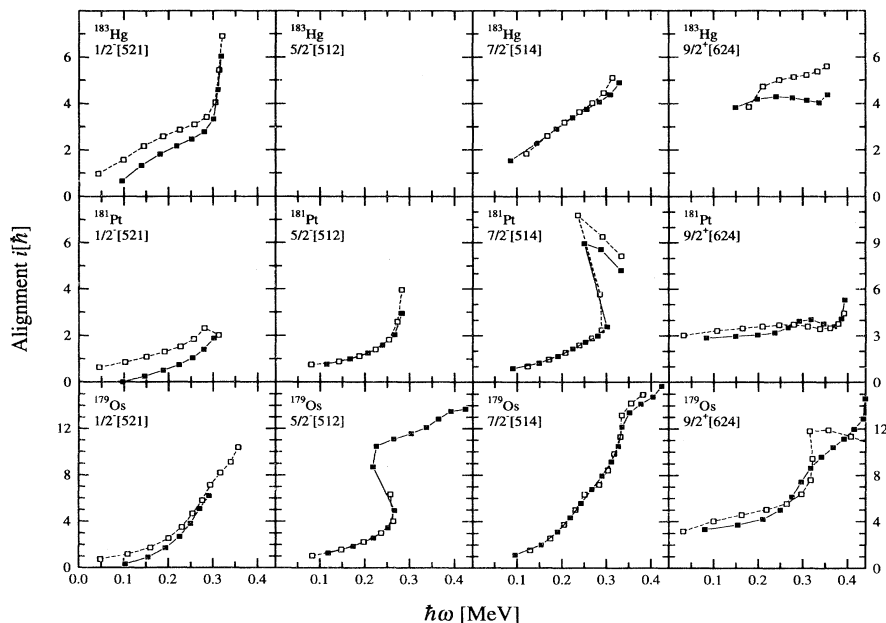


FIG. 4. Aligned angular momenta  $i$  of the bands in  $^{183}\text{Hg}$  are compared with those of the  $N = 103$  isotones  $^{181}\text{Pt}$  [6] and  $^{179}\text{Os}$  [7]. The open squares represent the favored signature. The reference parameters of  $J_0 = 22.5 \hbar^2/(\text{MeV})$  and  $J_1 = 180.0 \hbar^4/(\text{MeV})^3$  are used for  $^{183}\text{Hg}$ .

coupling formula [8] for the  $7/2^-$ [514] and  $5/2^-$ [512] bands. The intrinsic  $g_K$  factors were calculated from the Woods-Saxon single particle wave functions by using  $g_s = 0.70g_s^{\text{free}}$ , to be  $g_K = +0.29$  and  $-0.42$  for the  $7/2^-$ [514] and  $5/2^-$ [512] orbitals, respectively. Further-

more, the simple estimate  $g_R = Z/A = 0.437$  was used for the core  $g$  factor, and  $Q_0 = 7.8$  b was calculated from the deformation (using  $\beta_2 = 0.26$  from Ref. [4]). As shown in Fig. 5, the  $B(M1)/B(E2)$  ratios calculated for pure  $7/2^-$ [514] bands are much smaller than the experimental values, while the calculated ratios for the  $5/2^-$ [512] bands are much larger. Note that using a smaller value for  $g_R$ , say 0.30, would only increase the difference between these simple estimates and the data, because  $B(M1) \sim (g_K - g_R)^2$ . A strong Coriolis mixing between these bands would be able to account for the  $B(M1)/B(E2)$  ratios, but this would require that the  $5/2^-$ [512] bands must lie close in energy to the assigned  $7/2^-$ [514] bands since the Coriolis matrix element between these orbitals is rather weak. Experimentally, nearly degenerate  $5/2^-$ [512] and  $7/2^-$ [514] bands have been observed in both  $^{181}\text{Pt}$  [6] and  $^{179}\text{Os}$  [7], and strong mixing between these bands was invoked to explain the  $B(M1)/B(E2)$  ratios of the  $7/2^-$ [514] bands in  $^{179}\text{Os}$  [7]. Whether the strong Coriolis mixing suggested by the  $B(M1)/B(E2)$  ratios is also present in the  $7/2^-$ [514] band in  $^{185}\text{Hg}$  is an interesting and open question.

In summary, a pair of new bands with strong signature splitting have been established in  $^{183}\text{Hg}$ , and are assigned as the  $1/2^-$ [521] ground-state configuration. The experimental  $B(M1)/B(E2)$  ratios in the previously assigned  $7/2^-$ [514] bands suggest Coriolis mixing with unobserved  $5/2^-$ [512] bands. The  $9/2^+$ [624] bands decay directly to a low-lying  $13/2^+$  state with unknown excitation energy which is associated with an oblate shape; no excited members of the oblate band has been found. Further work is needed to confirm the spins and parities of the bandheads.

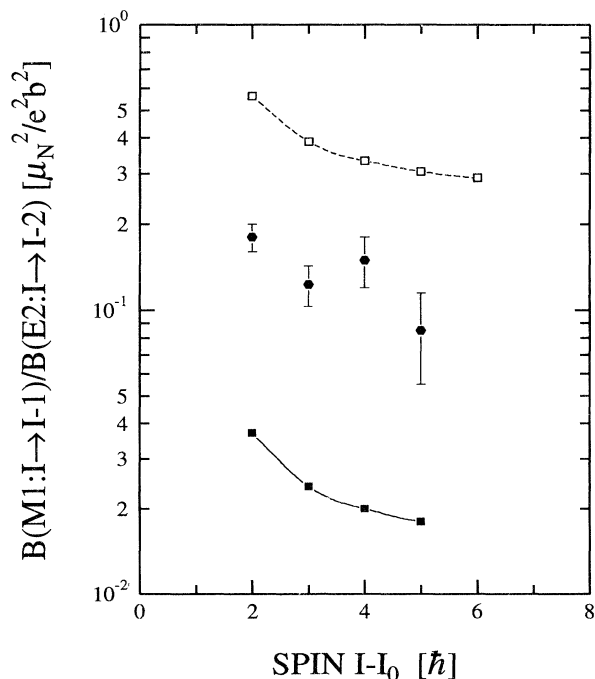


FIG. 5. The  $B(M1)/B(E2)$  experimental ratios as a function of the spins of the initial states for bands 3 and 4 and their  $\Delta I = 1$  interband transitions. The solid and dashed lines give the calculated ratios assuming a  $7/2^-$ [514] and a  $5/2^-$ [512] band assignment, respectively. The horizontal axis is  $I - I_0$  where the  $I_0$  is the bandhead spin. See text for detailed discussion.

Work at Vanderbilt University was supported by the U.S. DOE under Grant No. DE-FG05-88ER40407, at Florida State University by U.S. NSF under Grant No.

PHY-9210082 and at Tennessee Technological University by the U.S. DOE Grant No. DE-FG05-92ER40694. One of the authors (W.C.M.) would like to thank the College of Arts and Sciences, Mississippi State University for the

support during the course of this work. We are grateful to Dr. J.X. Saladin whose loan of the University of Pittsburgh detectors and electronics made the combined Pittsburgh-FSU detector array possible.

- 
- [1] J.H. Hamilton, in *Treatise on Heavy-Ion Science*, Vol. 8, edited by D.A. Bromley (Plenum, New York, 1989), p. 1, and references therein; G.D. Dracoulis, A.E. Stuchbery, A.O. Macchiavelli, C.W. Beausang, J. Burde, M.A. Deleplanque, R.M. Diamond, and F.S. Stephens, *Phys. Lett. B* **208**, 365 (1988).
- [2] G. Ulm, S.K. Bhattacharjee, P. Dabkiewicz, G. Huber, H.-J. Kluge, T. Kühn, H. Lochmann, E.-W. Otten, K. Wendt, S.A. Ahmad, W. Klempt, R. Neugart, and the ISOLDE Collaboration, *Z. Phys. A* **325**, 247 (1986), and references therein.
- [3] F. Hannachi, G. Bastin, M.G. Porquet, J.P. Thibaud, C. Bourgeois, L. Hildingsson, N. Perrin, H. Sergolle, F.A. Beck, and J.C. Merdinger, *Z. Phys. A* **330**, 15 (1988).
- [4] K.S. Bindra, A.V. Ramayya, W.C. Ma, B.R.S. Babu, J.H. Hamilton, L. Chaturvedi, J. Kormicki, R.V.F. Janssens, C.N. Davids, I. Ahmad, I.G. Bearden, M.P. Carpenter, W. Chung, D. Henderson, R.G. Henry, T.L. Khoo, T. Lauritsen, Y. Liang, H. Penttila, F. Soramel, C. Baktash, W. Nazarewicz, and J.A. Sheikh, *Phys. Lett. B* **318**, 41 (1993).
- [5] J. Bonn, G. Huber, H.-J. Kluge, L. Kugler, and E.-W. Otten, *Phys. Lett.* **38B**, 308 (1972); R.B. Firestone, *Nucl. Data Sheets* **52**, 715 (1987).
- [6] M.J.A. De Voigt, R. Kaczarowski, H.J. Riezebos, R.F. Noorman, J.C. Bacelar, M.A. Deleplanque, R.M. Diamond, and F.S. Stephens, *Nucl. Phys.* **A507**, 447 (1990).
- [7] J. Burde, M.A. Deleplanque, R.M. Diamond, A.O. Macchiavelli, F.S. Stephens, and C.W. Beausang, *Phys. Rev. C* **46**, 1642 (1992).
- [8] A. Bohr and B.R. Mottelson, *Nuclear Structure*, Vol. II (Benjamin, New York, 1975).